

The vascular morphology of melanoma is related to Breslow index: an in vivo study with dynamic optical coherence tomography

Nathalie De Carvalho, Julia Welzel, Sandra Schuh, Lotte Themstrup, Martina Ulrich, Gregor B. E. Jemec, Jon Holmes, Shaniko Kaleci, Johanna Chester, Laura Bigi, Silvana Ciardo, Giovanni Pellacani

Angaben zur Veröffentlichung / Publication details:

De Carvalho, Nathalie, Julia Welzel, Sandra Schuh, Lotte Themstrup, Martina Ulrich, Gregor B. E. Jemec, Jon Holmes, et al. 2018. "The vascular morphology of melanoma is related to Breslow index: an in vivo study with dynamic optical coherence tomography." *Experimental Dermatology* 27 (11): 1280–86. <https://doi.org/10.1111/exd.13783>.

Nutzungsbedingungen / Terms of use:

licgercopyright

Dieses Dokument wird unter folgenden Bedingungen zur Verfügung gestellt: / This document is made available under these conditions:



Deutsches Urheberrecht

Weitere Informationen finden Sie unter: / For more information see:

<https://www.uni-augsburg.de/de/organisation/bibliothek/publizieren-zitieren-archivieren/publiz/>



The vascular morphology of melanoma is related to Breslow index: An in vivo study with dynamic optical coherence tomography

Nathalie De Carvalho¹  | Julia Welzel² | Sandra Schuh² | Lotte Themstrup^{3,4}  |
Martina Ulrich⁵ | Gregor B. E. Jemec^{3,4} | Jon Holmes⁶ | Shaniko Kaleci¹ |
Johanna Chester¹ | Laura Bigi¹ | Silvana Ciardo¹ | Giovanni Pellacani¹

¹Department of Dermatology, University of Modena and Reggio Emilia, Modena, Italy

²Department of Dermatology, General Hospital Augsburg, Augsburg, Germany

³Department of Dermatology, Zealand University Hospital, Roskilde, Denmark

⁴Health Sciences Faculty, University of Copenhagen, Copenhagen, Denmark

⁵CMB Collegium Medicum Berlin, Berlin, Germany

⁶Michelson Diagnostics, Maidstone, UK

Correspondence

Nathalie De Carvalho, Department of Dermatology, University of Modena and Reggio Emilia, Modena, Italy.
Email: drnathaliedecarvalho@gmail.com

Funding information

The study has been fully funded by the European Union CIP-ICT PSP PROGRAMME GA N. 621015 ADVANCE.

Abstract

Background: Malignant melanoma is an aggressive skin cancer, which can lead to metastasis development. Vascularization enhancement is fundamental for tumor growth, worsening the prognosis. Dynamic optical coherence tomography (D-OCT) enables the in vivo evaluation of vascular patterns in skin lesions.

Objective: In vivo evaluation of the melanoma vessel morphology by means of D-OCT and correlation with Breslow index.

Methods: Retrospective analysis of histologically proven melanomas, evaluated by D-OCT at three different depths (150, 300 and 500 μm), was performed. Vessels were classified according to morphology (dots, blobs, coiled, line, curved, serpiginous), distribution (regular, irregular) and the presence/type of branches. The data were correlated with Breslow thickness.

Results: A total of 127 melanomas were evaluated. Dotted vessels were recorded at all depths, and their irregular distribution was associated with lesions thicker than 1.0 mm (from 75% to 91%), compared with thin ones (42%) at 150 μm ($P = 0.031$), and from 33% to 57% vs 18% at 300 μm ($P = 0.021$). Serpiginous and branching vessels with bulges were predominantly seen in melanomas thicker than 2 mm at 150 μm (from 14% to 27%, $P < 0.001$) and 300 μm of depth (from 36% to 54%, $P < 0.001$).

Limitations: Background noise hampered vessel detection at 500 μm . No correlation with dermoscopy/histology.

Conclusion: Vascular pattern evaluation at 150 and 300 μm provided data on tumor microvascular asset and its pattern of progression in accordance with Breslow thickness. Since vascular progression is theoretically linked with tumor aggressiveness, the study of vascular pattern related with melanoma metastatization capability is warranted.

KEYWORDS

dynamic OCT, melanoma, metastatization, neovascularization, tumor growth

1 | INTRODUCTION

Cutaneous melanoma is responsible for up to 90% of deaths associated with skin malignancies.^[1] Disease staging is dependent on tumor thickness, reported by histology according to the Breslow index,^[2] and is strongly correlated with patient prognosis; thicker lesions are correlated with worse outcomes and lower survival rates.

Neoangiogenesis is crucial for tumor progression and has been associated with metastasis and poor prognosis.^[3,4] Melanoma microcirculation seems dependent on promoting factors, such as vascular endothelial growth factor (VEGF) and tissue factor (TF),^[5] which are related to tumor growth and remodelling.^[6] Neoangiogenesis (the growth of new vessels) results in nourishing tumor cells with nutrients and oxygen, thereby promoting tumor growth. According to Schumacker et al., oxygen arrives to a limited depth of 100–150 μm .^[7] Beyond that depth, the intratumoral hypoxia leads to a consequent activation of hypoxia-inducible factor 1 (HIF1), which is a strong inducer of other angiogenic factors, enhancing the risk of metastasis.^[8,9] So ongoing tumor growth requires new vessels, and this explains why tumor vessels grow tightly together, rarely exceeding a distance of 0.2 to 0.3 micrometre from each other.^[7]

Three models for the interaction of melanoma and microvasculature have been proposed: vascular mimicry, vascular co-option and stimulation of bone marrow.^[10] The term *vascular mimicry* is used to describe the plasticity of aggressive cancer cells to create new vascular networks induced by hypoxia.^[11,12] In this mechanism, angiogenesis-promoting factors stimulate melanoma cells to invade the endothelial normal network and assume endothelial cell functions.^[13] *Vascular co-option* is the growth of tumor cells along pre-existing vessels.^[14] *The stimulation of bone marrow* is a mechanism by which tumor hypoxia induces the release of normal vascular progenitor cells to become components of the vascular network.^[15,16] The characteristics of melanoma microvascularization are therefore a consequence of tumor growth and thickness.

Optical coherence tomography (OCT) is a noninvasive imaging tool that provides transversal and enface images of the skin with a penetration depth of up to 1.5 mm and a resolution of 3 to 15 μm .^[17] Recently, dynamic optical coherence tomography (D-OCT) has been introduced as a supplementary noninvasive, novel imaging technique that allows the study of vessels in transversal and en face/horizontal sections in real time, creating images of the skin microangiography^[18–20] in superficial and deep dermal components (up to a depth of 0.5 mm). D-OCT principles rely on detecting motion of blood cells during structural OCT scans. A combined image of structural OCT is generated (depicting the tissue structure) together with D-OCT (highlighting the blood vessel structures). The relationship between vascular and tissue characteristics is emphasized.^[19]

Previous studies regarding the in vivo evaluation of the vascular characteristics with D-OCT in healthy skin and different skin conditions have already been done.^[19–22] In the field of skin cancer, D-OCT showed to be helpful in the differentiation between actinic keratosis (AK), Bowen's disease (BD) and squamous cell

carcinoma (SCC), being the presence of blob vessels at the depth of 300 μm in favour of BD, whereas curved vessels were predominantly seen in AK.^[23] Regarding basal cell carcinomas (BCC), some vascular characteristics showed to be helpful in classifying the subtype of this skin cancer, as proposed by Themstrup et al.^[24] In this study, it was shown that the presence of serpiginous vessels at the depth of 300 μm and 500 μm increased the risk of nodular BCC mainly if those vessels were branching at 300 μm . At the same time, their presence reduced the risk of the superficial subtype. Moreover, in nodular BCC, vessels displayed a circumscribed figure at the depth of 500 μm .

As differences in architectural transformation and disarray of microvasculature at D-OCT between melanoma and naevus have already been outlined,^[18] and the terminology for the study of the skin vascularization with D-OCT has also recently been proposed,^[19] the authors aimed to investigate whether in vivo evaluation with D-OCT of melanoma vascular characteristics is associated with Breslow index.

2 | METHODS

From June 2015 to April 2016, four European clinical dermatology centres were involved in a European Union-funded project (ADVANCE, Project No. 621015) and obtained ethics approval for the study from the respective institutional review boards. All patients were >18 years and gave written informed consent in accordance with the Declaration of Helsinki.

Lesions with clinical and/or dermoscopic aspects suggestive of melanoma were referred to D-OCT imaging prior to excision and histopathology. Images were prospectively collected and stored in a dedicated database. Lesions with sufficient quality D-OCT images and confirmed diagnosis by histopathology of primary melanoma with a specified Breslow thickness were included in the current study.

All lesions were assessed with the VivoSight® D-OCT (Michelson Diagnostics Ltd, Maidstone Kent, UK). The device scans a “multi slice” area of 6 × 6 mm comprising 120 cross-sectional/transversal OCT images of 6 mm width with an optical resolution of 7.5 μm in the lateral direction and 5 μm in the axial direction.

D-OCT image acquisition was performed as follows. The VivoSight OCT probe was placed gently but firmly onto the lesion, using the integrated colour camera to position the scan centrally on the lesion or, in case of asymmetric distribution of tumor growth, centrally on the nodular portion of the lesion. At this point, the correct focal distance was confirmed by viewing the live OCT image; if the skin surface was too high or too low, then the probe was removed and fitted with a lens spacer of a different size. (No refractive index matching gel was used as it is not necessary to obtain good images with the VivoSight device.) When ready, the probe button is actuated and the device scans a 6 × 6 mm square area of tissue in approximately 30 seconds during which the probe must be held steady to avoid motion artifacts.

To assess vessel morphology, the en face D-OCT images captured by the VivoSight were visually assessed. The en face images provided automatically by the VivoSight processing software. Each scan comprised 120 vertical D-OCT images, 6 mm wide by 2 mm deep, with a spacing of 0.05 mm so that the whole comprised a 3-D data block $6 \times 6 \times 2$ mm. The VivoSight software displayed a top-view horizontal slice at a user-selected depth below the skin surface, adjusted to compensate for the varying skin surface topography across the scanned region. The enface image display comprised the standard (structural) OCT data at the selected depth, with a red overlay representing the detected movement from blood flow from the vessels at that depth; the intensity of the red colour corresponded to the strength of the D-OCT signal. The D-OCT signal measures the strength of the detected blood flow using a proprietary algorithm based on speckle variance methods.^[25]

In this study, each lesion was scanned by D-OCT at the respective collaborating centre where primary assessment was performed. Lesions were scanned in the central area, and their vascular characteristics were evaluated in the horizontal/en face view. In order to extend the depth of assessment, an OCT Fitter software was used to provide horizontal D-OCT images at selected depths.^[26] Each lesion was examined at three depths of 150, 300 and 500 μm .

All D-OCT en face/horizontal images were reviewed by three dermatologists (NDC, SS and JW), all experts in D-OCT image assessment and blinded to the Breslow thickness index and any other clinical information. Evaluations were performed in blind on two separate monitors by NDC and SS, and in case of discordance, a third expert was called to supervise in order to take an agreed decision. At each of the three depths, the vascular morphology of each lesion was assessed according to Ulrich's classification.^[19,27] The vascular morphologies included *dots* (red small pinpoints), classified as *regular distribution* (a uniform distribution throughout the frame) or *irregular distribution* (unevenly distributed throughout the frame); *blobs* (large, red, circular structures); *coiled* (short, curled lines); *lines* (straight vessels); *curved* (lines forming semicircular shapes); *serpiginous* (waved line vessels); and *branching* (vessels forking from the main structure) sub-classified as *arborizing* (with progressively thinner branching) or *bulging* (dilated, aneurismatic-like areas) (Figure S1). Any vascular morphology was considered present when visualized at least three times in a single frame.

Lesions were grouped for analysis into five subgroups according to melanoma Breslow thickness^[1,28,29]: group 0 (in situ), group I (≤ 1 mm), group II (>1 , ≤ 2 mm), group III (>2 , ≤ 4 mm) and group IV (>4.0 mm). Associations between vascular morphologies and Breslow thickness were analysed.

2.1 | Statistics

The frequency of the vascular morphologies was calculated and compared between groups by Pearson's chi-square test and Fisher's exact test. Statistical analysis was performed using STATA[®] software version 14 (StataCorp. 2015. Stata Statistical Software: Release 14.

College Station, TX: StataCorp LP.). For all tests, a $P < 0.05$ was considered statistically significant.

3 | RESULTS

A total of 127 lesions, with Fitzpatrick skin phototypes varying from 1 to 3, were included in the current study. Eighty-six patients were male and 41 female. Age varied from 41 to 95 years. Lesions were located on the head/neck ($n = 26$), on the trunk ($n = 71$), on the lower limbs ($n = 17$), on the upper limbs ($n = 10$), on the soles of the foot ($n = 2$) and on the penile shaft ($n = 1$).

Lesions' Breslow thickness ranged from 0 (in situ) to 13 mm. Lesion diagnoses included 35 in situ melanoma (27.6%; group 0), 62 melanoma ≤ 1 mm (48.8%; group I), 12 melanoma > 1 and ≤ 2 mm (9.4%; group II), 11 melanoma > 2 and ≤ 4 mm (8.7%; group III) and 7 melanoma > 4 mm (5.5%; group IV). Figure 1 depicts the most characteristic D-OCT vascular patterns at 150 and 300 μm depth.

3.1 | Vascular morphologies at 150 μm depth

At the depth of 150 μm , the distribution of dotted vessels and the presence of coiled, curved, and serpiginous vessels were significantly different among the five melanoma subgroups, as seen in Table 1. In detail, dotted vessels were present in almost all lesions (99.2%). Concerning the distribution of dots, thin melanomas (subgroups 0 and I) displayed a regular pattern (58.3% and 55.7%, respectively) (Figure 1A,C), whereas an irregular distribution was more frequently identified in thicker lesions (75% in subgroup II, 90.9% in subgroup III and 85.7% in subgroup IV; $P = 0.031$) (Figure 1E,G,I). Coiled vessels were mainly visible in thicker lesions ($P = 0.011$), precisely in 18.2% of subgroup III and in 14.3% of subgroup IV compared to 0%-1.6% in subgroups 0-II. The presence of curved vessels was significantly different ($P = 0.004$) with a peak of presentation in subgroups II and III (33.3% and 54.5%, respectively). Serpiginous vessels and bulging branches were present in thicker lesions only (27.3% of group III and 14.3% of group IV; $P < 0.001$) (Figure 1G,I). Blobs and lines did not correlate with the melanoma thickness ($P = 0.359$).

3.2 | Vascular morphologies at 300 μm depth

At the depth of 300 μm , the distribution of dotted vessels, the presence of serpiginous vessels and branching significantly differed among the groups, as outlined in Table 1. Dotted vessels were present in all cases (100%), but an irregular distribution was more frequently related to increasing Breslow depth ($P = 0.021$). Serpiginous vessels were only observed in lesions thicker than 2 mm (54.5% of groups III and 42.9% of group IV; $P < 0.001$) (Figure 1H,J).

Concerning branching, arborizing vessels were more frequently observed in in situ and thick lesions (groups 0, III and IV), whereas bulging vessels were exclusively observed in lesions >1 mm, increasing in frequency according with Breslow thickness ($P < 0.001$) (Figure 1H,J).

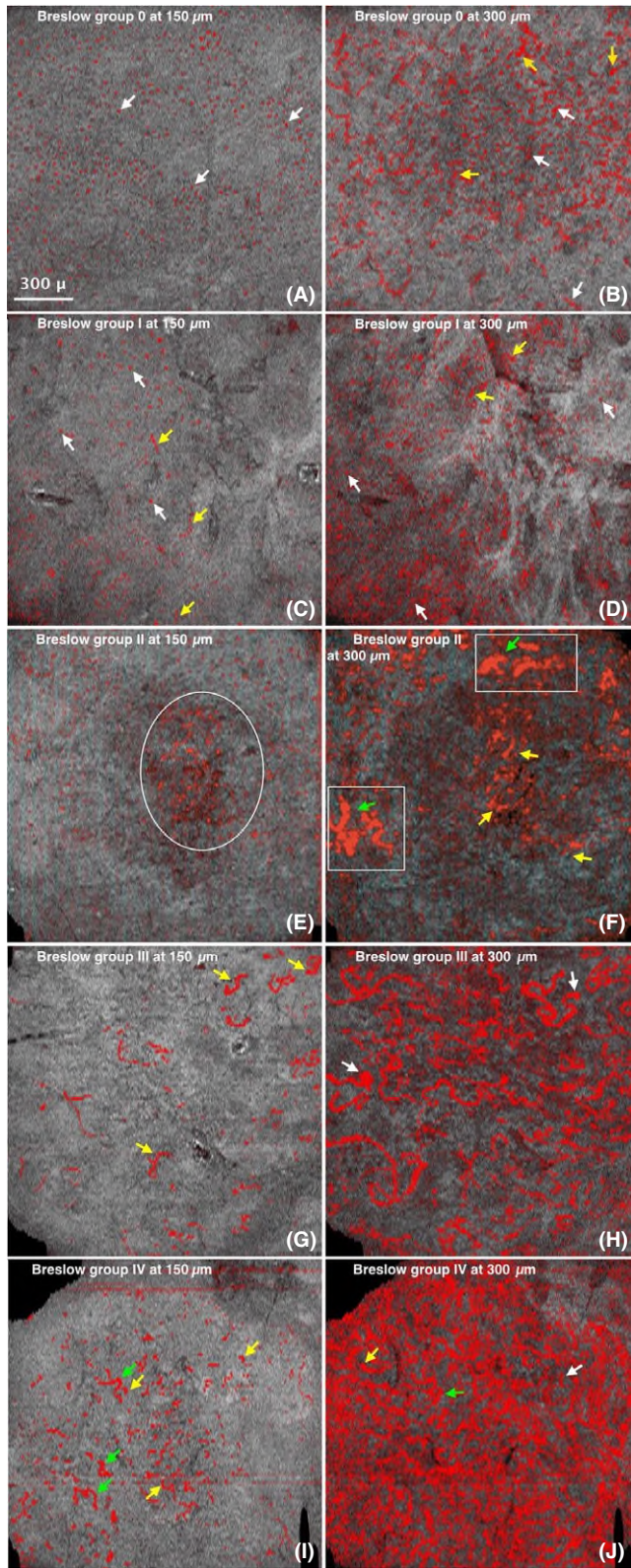


FIGURE 1 In vivo D-OCT evaluation of the grading of the microvasculature of melanomas according to Breslow thickness at the depth of 150 and 300 μm . (A) Melanoma in situ, classified into group 0, shows numerous dotted vessels regularly distributed throughout the lesion (white arrows) at the depth of 150 μm , and (B) same lesion at 300 μm depth shows regular distribution of dotted vessels mainly in the centre of the lesion, and few line vessels (white arrows) and curved vessels (yellow arrows). (C) Melanoma 0.9 mm, classified into group I, shows regularly distributed dotted vessels throughout the lesion (white arrows) and the presence of line vessels (yellow arrows), and (D) same lesion at 300 μm depth shows vascular pleomorphism with the presence of irregularly distributed dotted vessels (white arrow) and numerous line vessels (yellow arrows). (E) Melanoma 1.8 mm classified into group II displays an irregular distribution of dotted vessels, grouped in the central part of the image (white circle), and (F) same lesion at 300 μm depth shows linear vessels (yellow arrows) and curved vessels (white squares). Some vessels also show evident dilatation of their calibre, with bulging branches (green arrows). (G) Melanoma 3.2 mm, classified into group III, shows few dotted vessels and a predominance of serpiginous vessels (yellow arrows), and (H) same lesion at 300 μm depth shows evident bulging vessels, represented by dilated buds on the side of the vessels (white arrows). (I) Melanoma 4.0 mm, classified into group IV, shows irregular dotted vessels, curved vessels (yellow arrows) and serpiginous vessels (white arrows), and (J) same lesion at 300 μm depth shows an intense vascularization, characterized by branching vessels (white arrow)

4 | DISCUSSION

Melanoma is an aggressive tumor with potential to metastasize. Histopathological examination remains the golden standard for diagnosis and provides core data for the prognosis.^[3,4] The three main histological features that influence the prognosis of the melanoma are dermal invasion and tumor thickness (Breslow index), the presence of microscopic ulceration and mitotic rate.^[1,30] In contrast to other solid tumors, tumor angiogenesis is not currently considered a prognostic factor for cutaneous melanoma. Nevertheless, microvasculature may also play a role in the evolution of melanoma.^[31]

The peripheral area of melanoma lesions has been proven to be composed of typical capillaries derived from pre-existing vessels, whereas in the central portion of the tumor, vessels are in part generated by tumor cells during the process of vasculogenic mimicry.^[3,32] Therefore, D-OCT images were captured in the central area of flat lesions, in order to better identify in vivo effects of the neoangiogenesis. Instead, in case of elevated/palpable and nodular lesions, the D-OCT acquisition was properly done in those areas since they were the most representative areas of vasculature.

Thus, the study of vascular morphological changes as tumor progresses may provide useful information to understand the mechanism of invasion and metastasizing, as well as to provide important prognostic clues. D-OCT enables rapid in vivo, noninvasive visualization of the microvascular architecture of the skin, and was therefore used in this study to evaluate specific vascular morphologies, which were detected at different depths in histologically confirmed melanomas.

3.3 | Vascular morphologies at 500 μm depth

At the depth of 500 μm , serpiginous vessels were predominant in thicker lesion groups (groups III and IV; $P < 0.05$), whereas bulging vessels were predominantly seen in the thickest lesions (group IV; $P < 0.001$).

TABLE 1 Vascular morphology as visualized at D-OCT related to Breslow thickness at the depth of 150 and 300 μm . Group 0 (in situ melanoma), group I (≤ 1 mm), group II (>1 and ≤ 2 mm), group III (>2 and ≤ 4 mm) and group IV (>4.0 mm)

		Breslow Group (150 μm)									
		0 (36 lesions)		I (61 lesions)		II (12 lesions)		III (11 lesions)			IV (7 lesions)
Vascular morphology	N	%	N	%	N	%	N	%	N	%	P value
Dot Dist.											
Regular	21	58.3	34	55.7	3	25.0	1	9.1	1	14.3	0.031
Irregular	15	41.7	26	42.6	9	75.0	10	90.9	6	85.7	
Blob	2	5.6	12	19.7	3	25.0	2	18.2	1	14.3	0.359
Coiled	0	0.0	1	1.6	0	0.0	2	18.2	1	14.3	0.011
Line	4	11.1	6	9.8	1	8.3	1	9.1	0	0.0	0.928
Curved	4	11.1	7	11.5	4	33.3	6	54.5	1	14.3	0.004
Serpiginous	0	0.0	0	0.0	0	0.0	3	27.3	1	14.3	<0.001
Branching											
Arborizing	0	0.0	0	0.0	0	0.0	0	0.0	0	0.0	<0.001
Bulging	0	0.0	0	0.0	0	0.0	3	27.3	1	14.3	
		Breslow group (300 μm)									
		0 (36 lesions)		I (61 lesions)		II (12 lesions)		III (11 lesions)		IV (7 lesions)	
Vascular morphology	N	%	N	%	N	%	N	%	N	%	P value
Dot Dist.											
Regular	29	80.6	50	82.0	8	66.7	5	45.5	3	42.9	0.021
Irregular	7	19.4	11	18.0	4	33.3	6	54.5	4	57.1	
Blob	4	11.1	15	24.6	5	41.7	4	36.4	2	28.6	0.171
Coiled	14	38.9	19	31.1	6	50.0	7	63.6	5	71.4	0.094
Line	21	58.3	23	37.7	4	33.3	5	45.5	2	28.6	0.266
Curved	24	66.7	35	57.4	3	25.0	7	63.6	6	85.7	0.065
Serpiginous	5	13.9	4	6.6	2	16.7	6	54.5	3	42.9	<0.001
Branching											
Arborizing	10	27.8	5	8.2	1	8.3	3	27.3	1	14.3	<0.001
Bulging	0	0.0	0	0.0	1	8.3	4	36.4	3	42.9	

Dot Dist., distribution of dotted vessels; group 0, in situ melanoma; group I, melanoma with Breslow thickness ≤ 1 mm; group II, melanoma with Breslow thickness >1 and ≤ 2 mm; group III, melanoma with Breslow thickness >2 and ≤ 4 mm; and group IV, melanoma with Breslow thickness >4.0 mm.

In agreement with the hypothesized relationship between microvasculature and melanoma, growth significant correlations were found. With the increasing Breslow stage and tumor thickness, dotted vessels became more irregularly distributed and other vascular morphologies appeared, such as curved vessels in melanomas > 1 mm, and coiled and serpiginous vessels in melanomas with Breslow thickness > 2.00 mm. Interestingly, early changes in vascular morphologies were already present at the most superficial depth (150 μm). We hypothesize that these vascular changes may be correlated with neoangiogenesis and vascular mimicry related with increased tumor burden and dermal invasion. On the other hand, thicker melanomas were characterized by the appearance of branches, mainly of bulging structures visible in deeper layers, which may correspond to aneurismatic vessels generated by a rapid and chaotic growth pattern.

There are however many other factors which may influence skin vascularization, such as body location (ie, facial skin is characterized by a different vascular architecture compared with other body sites), anatomy (ie, epidermis in palms and soles is thicker than in other areas), inflammatory diseases (ie, contemporary presence of rosacea or other inflammatory skin diseases), photodamage and chronologically aged skin, which may interfere with the evaluation of the vascular components at D-OCT imaging.^[19] Moreover, technical limitations, such as projection artifacts, which appear as vertical streaks below a vessel, caused by interference with the D-OCT signal from the tissue directly below a vessel, or by the blood flow in the vessel, may confuse the precise visualization of the vascular morphology, especially in deeper layers. Indeed, in this set of lesions, we observed that the evaluation of the vascular morphologies lost significance for all patterns at the depth of 500 μm , except for the presence of

Depth	VESSEL TYPE	Group 0 (in situ)	Group I (0.01-1.00 mm)	Group II (1.01-2.00 mm)	Group III (2.01-4.00)	Group IV (>4.00 mm)
150 µm	Dotted regular					
	Dotted irregular					
	Coiled					
	Curved					
	Serpiginous					
	Branching arborizing					
	Branching bulging					
300 µm	Dotted regular					
	Dotted irregular					
	Coiled					
	Curved					
	Serpiginous					
	Branching arborizing					
	Branching bulging					

FIGURE 2 Illustration of the results of the study showing the relevant in vivo vessel types (red coloured square) in correlation with each melanoma group (0, I, II, III and IV) at the depths of 150 and 300 µm

serpiginous vessels and branches. An explanation for the loss of vascular morphologies at this depth could be the different refractivity of the tissue and/or the abundant presence of pigment, in comparison with other epithelial tumors, such as basal cell carcinoma, actinic keratosis and squamous cell carcinoma. Another limitation of this study was the no correlation between the vascular morphologies detected by D-OCT and the visible vessels seen in dermoscopy and histology.

As in other neoplasm, tumor burden and depth are influencing vascular pattern and vessel size. Keratinizing tumors (ie, AK, BD and SCC), basal cell carcinoma and melanoma showed a more homogeneous vascular pattern (linear/serpiginous, dotted and/or blobs) when lesions were superficial, whereas in nodular and thicker ones, the vascular pattern was more chaotic/heterogeneous and frequently showed ramifications (arborizing/branching/bulgings).^[23]

D-OCT evaluation of keratinizing tumors and BCC showed more consistent/monomorphous vascular pattern. On the other hand, D-OCT evaluation in melanoma showed that the vascular patterns were more heterogeneous than those seen in keratinizing tumors and BCC, with a higher variability in thinner lesions and progressive changes in the vascular pattern according to the depth.

Although histopathology remains the gold standard for melanoma diagnosis and classification of Breslow thickness, our preliminary results suggest that D-OCT may be a tool to study the microvascular architecture in skin tumors, mainly to detect phenomena related with angiogenesis occurring in the superficial dermal layers of early invasive tumors. The evaluation of the vascular aspects provides reliably detectable patterns up to a depth of 300 µm. The overall finding of irregular distribution of dotted vessels at 150 µm and the progressive appearance of curved, coiled and serpiginous vessels followed by the detection of branched and bulging vessels observable at 300 µm can well describe the vascular changes during melanoma progression (Figure 2). The evaluation of vascular morphology in melanomas may prove a biomarker to estimate the tumor aggressiveness, and further studies seem justified to confirm the possibility of D-OCT to access tumor aggressiveness.

CONFLICT OF INTEREST

Jon Holmes is acting CEO and Chief Technology Officer at Michelson Diagnostics, the manufacturer of the D-OCT used in this study. The

other authors declare no conflict of interests. The authors declare that the manuscript contains original, unpublished work that is not being considered for publication elsewhere at this time. The study has been approved by the Ethics Committee of Modena (prot. N. 3184/CE, 25-AUG-2014). Informed consent was obtained from all patients.

AUTHOR CONTRIBUTION

N. De Carvalho, J. Welzel, S. Schuh, L. Themstrup, M. Ulrich, GBE. Jemec, J. Holmes, S. Kaleci, J. Chester, L. Bigi and S. Ciardo performed the research. G Pellacani and N. De Carvalho designed the research study. S. Kaleci analysed the data. N. De Carvalho and J. Chester wrote the paper.

ORCID

Nathalie De Carvalho  <http://orcid.org/0000-0002-0823-5731>

Lotte Themstrup  <http://orcid.org/0000-0003-1368-1522>

REFERENCES

- [1] C. Garbe, K. Peris, A. Hauschild, P. Saiag, M. Middleton, J. Bastholt, J. J. Grob, J. Malvehy, J. Newton-Bishop, A. J. Stratigos, H. Pehamberger, A. M. Eggermont, European Dermatology Forum (EDF), European Association of Dermato-Oncology (EADO), European Organisation for Research and Treatment of Cancer (EORTC), *Eur. J. Cancer* **2016**, 63, 201.
- [2] M. Watson, A. C. Geller, M. A. Tucker, G. P. Guy Jr, M. A. Weinstock, *Prev. Med.* **2016**, 91, 294.
- [3] V. Zidlik, S. Brychtova, M. Uvirova, D. Ziak, J. Dvorackova, *Int. J. Mol. Sci.* **2015**, 16, 7876.
- [4] R. R. Braeuer, I. R. Watson, C. J. Wu, A. K. Mobley, T. Kamiya, E. Shoshan, M. Bar-Eli, *Pigment Cell Melanoma Res.* **2014**, 27, 19.
- [5] A. Vartanian, E. Stepanova, I. Grigorieva, E. Solomko, A. Baryshnikov, M. Lichinitser, *Melanoma Res.* **2011**, 21, 91.
- [6] W. Ruf, E. A. Seftor, R. J. Petrovan, R. M. Weiss, L. M. Gruman, N. V. Margaryan, R. E. Seftor, Y. Miyagi, M. J. Hendrix, *Cancer Res.* **2003**, 63, 5381.
- [7] P. T. Schumacker, R. W. Samsel, *J. Appl. Physiol.* **1985**, 1989(67), 1234.
- [8] S. Meierjohann, *Front. Oncol.* **2015**, 5, 102.
- [9] A. Marconi, R. G. Borroni, F. Truzzi, C. Longo, F. Pistoni, G. Pellacani, C. Pincelli, *Exp. Dermatol.* **2015**, 24, 396.
- [10] M. Felcht, M. Thomas, *J. Dtsch. Dermatol. Ges.* **2015**, 13, 125.
- [11] R. K. Jain, *Nat. Med.* **2001**, 7, 987.
- [12] R. E. Seftor, A. R. Hess, E. A. Seftor, D. A. Kirschmann, K. M. Hardy, N. V. Margaryan, M. J. Hendrix, *Am. J. Pathol.* **2012**, 181, 1115.
- [13] A. J. Maniotis, R. Folberg, A. Hess, E. A. Seftor, L. M. Gardner, J. Pe'er, J. M. Trent, P. S. Meltzer, M. J. Hendrix, *Am. J. Pathol.* **1999**, 155, 739.
- [14] J. Welte, S. Loges, S. Dimmeler, P. Carmeliet, *J. Clin. Invest.* **2013**, 123, 3190.
- [15] G. Bergers, D. Hanahan, *Nat. Rev. Cancer* **2008**, 8, 592.
- [16] R. Du, K. V. Lu, C. Petritsch, P. Liu, R. Ganss, E. Passequé, H. Song, S. Vandenberg, R. S. Johnson, Z. Werb, G. Bergers, *Cancer Cell* **2008**, 13, 206.
- [17] J. Welzel, E. Lankenau, R. Birngruber, R. Engelhardt, *J. Am. Acad. Dermatol.* **1997**, 37, 958.

- [18] N. De Carvalho, S. Ciardo, A. M. Cesinaro, G. Jemec, M. Ulrich, J. Welzel, J. Holmes, G. Pellacani, *J. Eur. Acad. Venereol.* **2016**, 30, e67.
- [19] M. Ulrich, L. Themstrup, N. de Carvalho, M. Manfredi, C. Grana, S. Ciardo, R. Kästle, J. Holmes, R. Whitehead, G. B. Jemec, G. Pellacani, J. Welzel, *Dermatology* **2016**, 232, 298.
- [20] L. Themstrup, J. Welzel, S. Ciardo, R. Kaestle, M. Ulrich, J. Holmes, R. Whitehead, E. C. Sattler, N. Kindermann, G. Pellacani, G. B. Jemec, *Microvasc. Res.* **2016**, 107, 97.
- [21] S. Schuh, J. Holmes, M. Ulrich, L. Themstrup, G. B. E. Jemec, N. De Carvalho, G. Pellacani, J. Welzel, *Dermatol. Ther. (Heidelb)*. **2017**, 7, 187.
- [22] L. Themstrup, S. Ciardo, M. Manfredi, M. Ulrich, G. Pellacani, J. Welzel, G. B. Jemec, *J. Eur. Acad. Dermatol. Venereol.* **2016**, 30, 974.
- [23] L. Themstrup, G. Pellacani, J. Welzel, J. Holmes, G. B. E. Jemec, M. Ulrich, *J. Eur. Acad. Dermatol. Venereol.* **2017**, 31, 1655.
- [24] L. Themstrup, N. De Carvalho, S. M. Nielsen, J. Olsen, S. Ciardo, S. Schuh, B. M. Nørnberg, J. Welzel, M. Ulrich, G. Pellacani, G. B. E. Jemec, *Exp. Dermatol.* **2018**, 27, 156.
- [25] A. Mariampillai, B. A. Standish, E. H. Moriyama, M. Khurana, N. R. Munce, M. K. Leung, J. Jiang, A. Cable, B. C. Wilson, I. A. Vitkin, V. X. Yang, *Opt. Lett.* **2008**, 33, 1530.
- [26] M. Manfredi, C. Grana, G. Pellacani. Skin Surface Reconstruction and 3D Vessels Segmentation in Speckle Variance Optical Coherence Tomography. 11th Joint Conference on Computer Vision, Imaging and Graphics Theory and Applications (VISIGRAPP 2016) – Volume 4: Visap, pp. 234-240.
- [27] M. Ulrich, L. Themstrup, N. de Carvalho, S. Ciardo, J. Holmes, R. Whitehead, J. Welzel, G. B. E. Jemec, G. Pellacani, *J. Eur. Acad. Dermatol. Venereol.* **2018**, 32, 152.
- [28] A. Breslow, *Ann. Surg.* **1970**, 172, 902.
- [29] C. K. Bichakjian, A. C. Halpern, T. M. Johnson, A. Foote Hood, J. M. Grichnik, S. M. Swetter, H. Tsao, V. H. Barbosa, T. Y. Chuang, M. Duvic, V. C. Ho, A. J. Sober, K. R. Beutner, R. Bhushan, W. Smith Begolka, American Academy of Dermatology, *J. Am. Acad. Dermatol.* **1032**, 2011, 65.
- [30] G. Zamolo, F. Gruber, L. Cabrijan, V. Micović, Z. Iternicka, N. Jonjić, *Acta Med. Okayama* **2001**, 55, 289.
- [31] N. Weidner, *Am. J. Pathol.* **1995**, 147, 9.
- [32] S. Zhang, D. Zhang, B. Sun, *Cancer Lett.* **2007**, 254, 157.

SUPPORTING INFORMATION

Additional supporting information may be found online in the Supporting Information section at the end of the article.

Figure S1. Schematic illustration of the different vascular morphologies observed in D-OCT, as well as the distribution of dotted vessels and classification of branchings.

How to cite this article: De Carvalho N, Welzel J, Schuh S, et al. The vascular morphology of melanoma is related to Breslow index: An in vivo study with dynamic optical coherence tomography. *Exp Dermatol.* 2018;27:1280–1286. <https://doi.org/10.1111/exd.13783>